

# Mimics and diagnostic pitfalls of intracranial lesions in conventional MRI: Clues on advanced MRI

<sup>1,2</sup>Alan Basil Peter, <sup>1</sup>Norlisah Ramli, <sup>1</sup>Kartini Rahmat, <sup>1</sup>Faizatul Izza Rozalli, <sup>1</sup>Che Ahmad Azlan

<sup>1</sup>Department of Biomedical Imaging, University Malaya Research Imaging Centre, University of Malaya, Kuala Lumpur; <sup>2</sup>Universiti Teknologi MARA, Selangor, Malaysia

## Abstract

**Objective:** To delineate and differentiate between late subacute hemorrhage and intracranial lipomas in clinically available conventional and advanced MR sequences. **Methods:** Two cases of late subacute hemorrhage and two cases of intracranial lipoma were reviewed with CT scans and 3.0T scanner MRI. The sequences evaluated in MRI were T1-weighted (T1W) fast spin echo (FSE), T2-weighted (T2W) FSE, gradient echo T2\*-weighted (GRE T2\*W) images, diffusion weighted (DWI), apparent diffusion coefficient (ADC) and multivoxel spectroscopy. **Results:** Late subacute hemorrhage and intracranial lipoma have similar imaging features on T1W, T2W FSE with blooming artefact at the margins on GRE T2\*W. However on GRE T2\*W sequence, the central area of lipoma demonstrates low signal; while hemorrhage demonstrates high signal. In DWI, late subacute hemorrhage shows hyperintensity; while in lipoma there is loss of signal.

**Conclusion:** Awareness of the potential pitfalls in standard sequence are important, as these entities appear to have similar T1W/ T2W characteristic with blooming artefact on T2\*W. Knowing the distinctive central signal intensity pattern on GRE T2W\* and DWI is therefore essential to differentiate between these lesions as there are differences to their clinical management.

## INTRODUCTION

In MRI T1W sequence, with short time-to-repeat (TR) and short time-to-echo (TE), lesions with short T1 values are hyperintense. Examples of these lesions are fat that has a T1 value of approximately 200ms<sup>1</sup> and subacute hemorrhage due to the presence of paramagnetic methemoglobin that shortens the T1 relaxation time.

In T2W spin echo (SE) sequences (with long TR/TE and depends upon local dephasing of spins following the application of the RF pulse) fat would give lower signal to water. Fat having a shorter T2 (60ms) than water (2000ms)<sup>1</sup>, relaxes more rapidly than water. However, in most commercially available MRI, FSE (Fast Spin Echo) sequences are employed, as they provide conventional SE contrast for most tissues and result in several fold reduction in imaging time. Fat, which is known to show hyperintense signal on T1W SE and hypointense signal on conventional T2W SE sequences, but on FSE exhibits hyperintense signal on both T1W and T2W sequences. The hyperintense appearance

of fat in T2W FSE is caused by the application of rapid multiple refocusing radiofrequency (RF) pulses during imaging. The RF pulses break the J-coupling within the lipid molecules and cause fat containing tissues to have a longer T2 time and appear more hyperintense in FSE compared to conventional SE images.<sup>2</sup>

In late subacute hemorrhage, the hemoglobin is converted to methemoglobin in the extracellular compartment, which results in short T1 and long T2 times. Therefore, late subacute hemorrhage and intracranial lipoma have similar signal appearances on T1W and T2W FSE images.

The aim of this paper is to present a pictorial review of the potential mimics and pitfalls in employing standard FSE sequence to differentiate late subacute hemorrhage from intracranial lipoma given their similarities in imaging features and discusses the strategies to differentiate these entities.

## METHODS

We reviewed and describe the imaging presentations of 4 cases: 2 cases of late subacute hemorrhage

and 2 cases of intracranial lipoma. The CT scan was performed with a Siemens SOMATOM Definition Dual Source 64 slice scanner (Siemens Healthcare, Erlangen, Germany) and the MRIs were performed with the standard protocol in the General Electric Signa EXCITE 3.0T scanner using the Millennium III 8-channel neurovascular head coil (GE Healthcare, Waukesha, WI, USA). Set up protocol of T1W FSE, T2W FSE, T2\*W GRE, T2W FSE fat saturated, DWI, ADC and multivoxel spectroscopy are as follows:

T1W FSE (TR = 1257ms, TE = 5.9ms, FOV = 24mm, matrix = 512 x 320, slice thickness = 5mm and spacing = 1.5mm); T2W FSE (TR = 4600ms, TE = 99.0ms, FOV = 24mm, matrix = 512 x 384, slice thickness = 5mm and spacing = 1.5mm); GRE T2\*W (TR = 680ms, TE = 20.0ms, flip angle = 20°, FOV = 24mm, matrix = 320 x 256, slice thickness = 5.0mm and spacing = 1.5mm); T2 FSE fat saturated (TR = 2000ms, TE = 102.0ms, FOV = 18mm, matrix = 448 x 256, slice thickness = 3.5mm and spacing = 1.0mm), DWI (TR = 8000ms, TE = 73.0ms, FOV = 24mm, matrix = 128 x 192, slice thickness = 5mm and spacing = 1.5mm, b value = 1000s/mm<sup>2</sup>), ADC (TR = 8000ms, TE = 72.9ms, FOV = 260mm, matrix = 128 x 192, slice thickness = 5mm and spacing = 2.0mm, b value = 1000s/mm<sup>2</sup>) and multivoxel spectroscopy (TR = 1000ms, TE = 144.0ms, FOV = 18mm, matrix = 16 x 16 and voxel thickness = 10mm).

**RESULTS**

**Case 1 and 2: Late subacute hemorrhage**

A 34-year-old man presented with acute hydrocephalus, and upon insertion of an extraventricular drain (EVD), developed an intraparenchymal hemorrhage in the right parietal lobe seen along the EVD tract (Figure 1). Our second case is a 64-year-old man presented with right occipital lobe venous hemorrhage with left transverse and sigmoid sinus dural arteriovenous fistula with corticovenous reflux and venous hypertension (Figure 2). Both these hemorrhages became hypodense on follow up NECT imaging performed a few weeks later and showed hyperintense signal on T1W and T2W FSE images with a hypointense rim on T2\*W GRE sequence consistent with late subacute hemorrhage. DWI sequence demonstrates hyperintense signal with corresponding signal loss on ADC.

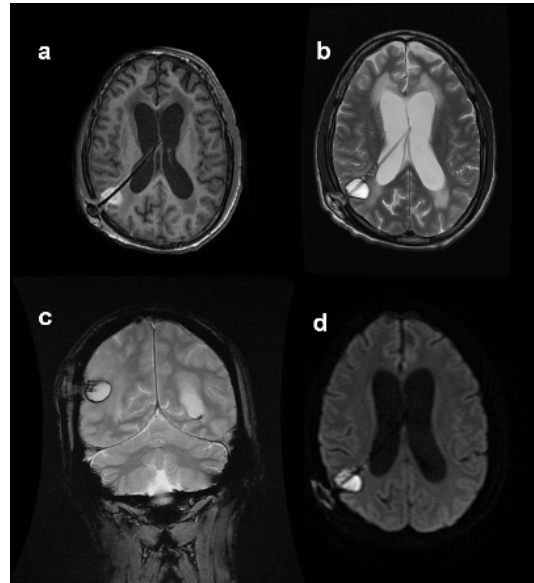


Figure 1. Case 1: 34 year old man with right parietal lobe intraparenchymal hemorrhage along the EVD tract. T1W FSE (Figure 1a), T2W FSE (Figure 1b) and DWI (Figure 1d) showed hyperintense bleed with hypointense rim on GRE T2\*W (Figure 1c) sequence.

**Case 3 and 4: Intracranial lipoma**

A 6-year-old girl with normal developmental milestones presented with unprovoked tonic seizures (Figure 3). She was initially misdiagnosed as having an inferior sagittal sinus thrombosis

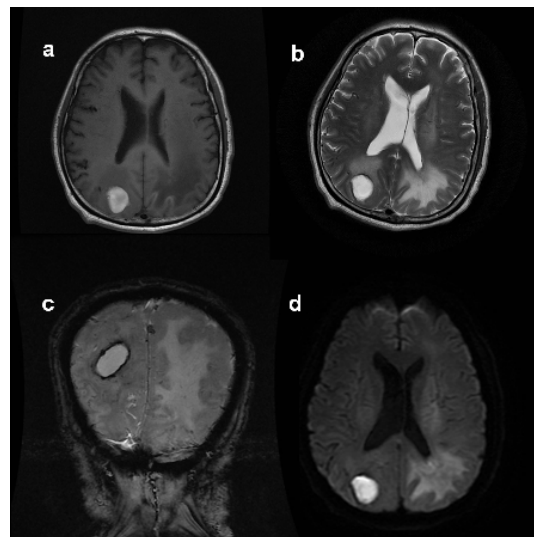


Figure 2. Case 2: 64 year old man with right occipital lobe venous hemorrhage. T1W FSE (Figure 2a), T2W FSE (Figure 2b) and DWI (Figure 2d) showed hyperintense bleed with hypointense rim on GRE T2\*W (Figure 2c) sequences.

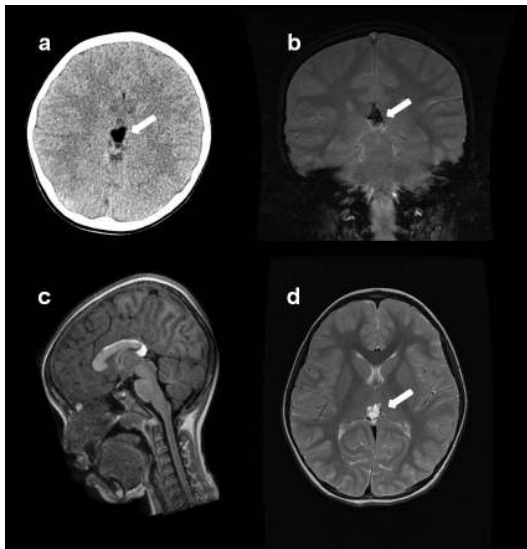


Figure 3. Case 3: 6 year old girl with pericallosal lipoma. NECT (Figure 3a) demonstrated a hypodense lesion. MRI GRE T2\*W sequence showed hypointense signal with blooming artefacts (Figure 3b) and hyperintense signal on MRI T1W FSE (Figure 3c) and T2W FSE (Figure 3d) images.

based on the T2\*W GRE; however, correlation made with the NECT scan of the brain showed a hypodense lesion in the pericallosal region with H.U. of -80 to -110 consistent with a pericallosal lipoma. On NECT scan imaging, the tumor appears as well circumscribed hypodense lesion with Hounsfield Unit (H.U.) of -50 to -100. Our second case of intracranial lipoma is a 70-year-old woman presented with symptoms of raised

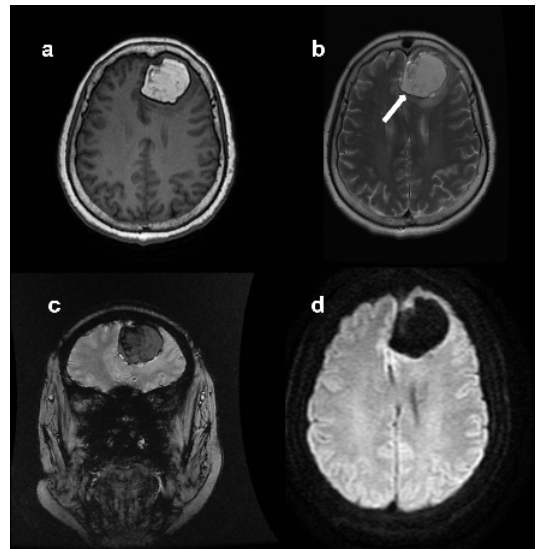


Figure 4. Case 4: 70 year old woman with left parafalcine lipoma. Hyperintense signal was revealed within the lipoma on T1W FSE (Figure 4a) and T2W FSE (Figure 4b). A dark band seen (arrow) depicting the chemical-shift artefact on the frequency encoding direction (Figure 4b). While on GRE T2\*W image, hypointense band seen outlining the lipoma with hypointense signal within (Figure 4c). Complete loss of signal on DWI sequences (Figure 4d).

intracranial pressure (Figure 4) and was found to have a parafalcine lipoma. The pericallosal and parafalcine lipoma both displayed hypointense signal and blooming artefacts on T2\*W GRE sequence, hyperintense signal on both T1W and T2W FSE images and demonstrated signal loss on

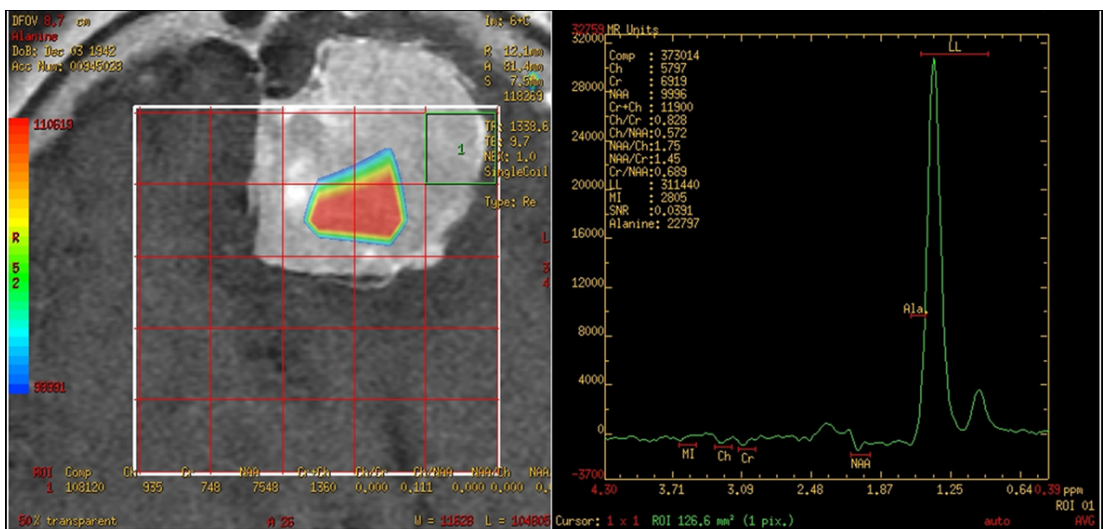


Figure 5. MR multivoxel spectroscopy of Case 4(left parafalcine lipoma) which demonstrates a lipid peak within 1.3 parts per million (ppm) range.

DWI. MR spectroscopy of the parafalcine lipoma demonstrated a high lipid peak at 1.3 parts per million (ppm) (Figure 5).

Summary and the differentiating MR findings of late subacute hemorrhage and intracranial lipoma and in T1W FSE, T2W FSE, GRE T2\*W images, DWI and ADC are presented in Table 1.

## DISCUSSION

Fat and blood are both hyperintense on T1W and T2W FSE sequences. Utilising only these conventional sequences in differentiating the cases illustrated above is therefore inadequate. The GRE sequence with T2\*W based contrast is normally used for detecting hemorrhage, calcification and iron deposition in various tissues.<sup>3</sup> Several articles have recommended T2\*W GRE sequence to differentiate between late subacute hemorrhage and intracranial lipoma.<sup>4,5</sup> As demonstrated in Cases 1 and 2, late (more than 7 days) subacute intracranial bleed/hemorrhage (methemoglobin) would typically show hyperintense signal on T1W and T2W FSE images, with hypointense signal or blooming artefacts on GRE T2\*W sequence. The GRE sequence deploys an RF pulse that partially flips the net magnetization vector into the transverse plane. MR echoes are produced by gradients, as opposed to RF pulses as in FSE. GRE sequences with long TE are T2\*W, in contrast with T2W as seen in spin echo sequences.<sup>6</sup> GRE T2\*W sequences are affected by magnetic field inhomogeneity which occurs at the interface between different tissues or entities; this gives rise to susceptibility artefacts.<sup>3</sup> This characteristic of the GRE T2\*W sequence is used for the detection of hemorrhage due to the susceptibility effect produced by iron and breakdown products of hemoglobin.

We also found that GRE T2\*W produces 'blooming artefacts' in the margin of both entities. The signal intensity is lower in GRE T2\*, as only spins that have been dephased by the action

of the gradient field are refocused. The loss of signal occurring in lipoma is likely to be due to the net effects of intravoxel chemical shift due to the difference of precession of fat and water within the lipoma itself. This is in contrast to the loss of signal occurring in methemoglobin that is due to magnetic field inhomogeneity.<sup>4,5</sup> As we have illustrated here, the differentiating feature lies in the central signal. Within lipoma, GRE sequence with T2\*W exhibits T2W SE sequence image characteristics rather than T2W FSE image characteristics, thus rendering fat (lipoma) hypointense on GRE T2\*W images. Whereas in late subacute hemorrhage, the central area of demonstrates high signal intensity in T2\*W GRE due to the proteinaceous material within the hemorrhage.

Lipoma (Cases 3 and 4) consist of mature fat cells and may exhibit chemical shift artefacts, which are due to different precessional frequency of <sup>1</sup>H protons in water and lipid tissues. There are two kinds of chemical shift artefacts that occur at fat-water interface. In the first kind, the artefact is seen as displacement of fat and the formation of dark and hyperintense bands at the interface of fat-water along the frequency encoding direction<sup>7,8</sup> as observed in parafalcine lipoma patient (Figure 4b). This type of chemical shift artefact could be minimized by reducing the FOV (field of view), increasing the receiver bandwidth and using a lower field MRI scanner.<sup>9</sup> The second kind of chemical shift artefact occurs only in GRE when lipid and water molecules are present in the same voxel of an MR image. If the phases of protons in water and lipid tissues are exactly opposite, their transverse magnetization will cancel each other out and the signal intensity in the voxel will be minimized.<sup>10</sup> The artefact is within the volume of the lipoma. However, unlike the first kind of chemical shift, the occurrence of this artefact is not restricted to the frequency encoding direction.<sup>9</sup> This artefact results in the black band surrounding the whole lipoma as seen in GRE T2\*W done with

**Table 1: MRI imaging characteristics of late subacute hemorrhage and intracranial lipoma**

Diagnosis	T1W (FSE)	T2W (FSE)	T2*W (GRE)	DWI	ADC
Late subacute hemorrhage	Increased signal	Increased signal	Blooming artefacts with central area of hyperintensity	Increased signal	Decreased signal
Lipoma	Increased signal	Increased signal	Blooming artefacts with central area of hypointensity	Loss of signal	Loss of signal

TE=20 ms, an out-of-phase image (Figure4c). This type of artefact could be minimized by using a suitable TE, which is dependent on the field strength of the scanner. Hence, the protons in water and lipid are in-phase during the signal readout.

DWI can further assist in the delineation of these entities. There is marked restricted diffusion in late subacute hematomas.<sup>11</sup> Since this sequence is part of most standard brain imaging protocols, the reporting radiologist is usually alerted to the possibility of sub acute hematoma by the striking diffusion restriction (hyperintense signal on DWI) seen in blood products. Other MRI sequences that may help to differentiate between late subacute hemorrhage and intracranial lipoma and would be MRI fat-saturated sequence, hemorrhage would not be suppressed in this sequence. Newer MRI sequences such as susceptibility-weighted imaging (SWI), which uses deoxyhemoglobin, ferritin and hemosiderin detection may have a potential role in differentiating between these two entities.<sup>12</sup> MR spectroscopy could also be useful as lipid, would demonstrate a high peak at 1.3 parts ppm, although it is a time-consuming and artefact prone technique.

In conclusion, awareness of the imaging appearances of late subacute hemorrhage and intracranial lipoma is important as the clinical management of these entities differ. These entities appear to have similar T1W, T2W and to a certain extent T2\*W characteristics on MRI. To distinguish between these entities, utilisation and careful evaluation of advanced sequences i.e. central signal in GRE T2\*W and the respective DWI imaging appearances is recommended.

## ACKNOWLEDGEMENT

The study was funded by the University of Malaya Research Grant RP008A-13HTM and was made possible by the University of Malaya Research Imaging Centre (UMRIC) resources.

## REFERENCES

1. Curry TS, Dowdey JE, Murry RC. Christensen's physics of diagnostic radiology. Lippincott Williams & Wilkins; 1990.
2. McRobbie DW, Moore EA, Graves MJ, Prince MR. MRI from picture to proton. Cambridge University Press; 2006.
3. Chavhan GB, Babyn PS, Thomas B, Shroff MM, Haacke EM. Principles, techniques, and applications of T2\*-based MR imaging and its special applications 1. *Radiographics* 2009;29(5):1433-49.
4. Jabot G, Stoquart-Elsankari S, Saliou G, Toussaint

- P, Deramond H, Lehmann P. Intracranial lipomas: clinical appearances on neuroimaging and clinical significance. *J Neurol* 2009;256(6):851-5.
5. Barkovich AJ. Section 1 Congenital Malformations: Lipoma. In: Osborn AG, Salzman KL, *et al*, eds: Diagnostic imaging. Baltimore: Amirsys, 2010: 1-1-22-25.
6. Bitar R, Leung G, Perng R, *et al*. MR pulse sequences: What every radiologist wants to know but is afraid to ask 1. *Radiographics* 2006;26(2):513-37.
7. Dietrich O, Reiser MF, Schoenberg SO. Artifacts in 3-T MRI: physical background and reduction strategies. *Eur J Radiol* 2008;65(1):29-35.
8. Herrick RC, Hayman LA, Taber KH, Diaz-Marchan PJ, Kuo MD. Artifacts and pitfalls in MR imaging of the orbit: a clinical review. *Radiographics* 1997;17(3):707-24.
9. Chavhan GB. MRI made easy. JP Medical Ltd; 2013.
10. Woodward P. MRI guide for technologists. McGraw-Hill; 1995.
11. Kang BK, Na DG, Ryoo JW, Byun HS, Roh HG, Pyeun YS. Diffusion-weighted MR imaging of intracerebral hemorrhage. *Korean J Radiology* 2001;2(4):183-91.
12. Haacke EM, Mittal S, Wu Z, Neelavalli J, Cheng YC. Susceptibility-weighted imaging: technical aspects and clinical applications, part 1. *Am J Neuroradiol* 2009;30(1):19-30.